

Development of a Magnetic Suspension Densimeter and Measurement of the Density of Toluene¹

R. Masui²

¹ Paper presented at the Fourteenth Symposium on Thermophysical Properties, June 25-30, 2000, Boulder, Colorado, U.S.A.

² Department of Thermal Metrology, National Research Laboratory of Metrology, Tsukuba 305-8563, Japan

Abstract

The development of a magnetic suspension densimeter that has been built for measurement of the density of compressed liquid at pressures up to 30MPa in the temperature range 20-150 °C is described. The densimeter was first built by the author and his coworkers at NIST. We describe here further improvements made on a second system built at NRLM based on the same principle.

The densimeter uses a small coil suspended from an electronic balance. Within the coil is placed a sample cell in which the pressurized sample and a buoy, which is a permanent magnet, is enclosed. For measurement of density, balance readings are recorded (1) with the buoy at rest, and (2) with the buoy in magnetic suspension. The measurement procedure is basically a hydrostatic weighing, which is simpler than those of conventional magnetic densimetry.

As an example, measurements of toluene density performed as part of an inter-laboratory comparison are presented. The data agreed with reliable literature values to within a few hundredths of a per cent.

KEY WORDS: compressed liquid; densimetry; density of liquid; electronic balance; magnetic densimeter; magnetic levitation; toluene; weighing

1 Introduction

Magnetic-suspension densimetry provides a direct and convenient way of measuring the density of pressurized liquids. A buoy made of magnetic material is suspended in the liquid by means of a magnetic field generated by a field coil. The density is derived from measurement of the force required to support the buoy.

Beams[1, 2], the pioneer of magnetic densimetry, and his coworkers have proposed two methods of measuring the buoyant force in magnetic densimetry. One is to measure the coil current necessary to support the buoy. The other is to suspend the sample cell from a balance, and to determine the change in weight of the cell as the buoy is brought into support.

The first method involves an accurate positioning of the buoy with respect to the coil, because the coil current is strongly dependent on the distance from the support coil. This can be elaborate work. Furthermore, changes in magnetization of the buoy as a function of temperature have to be calibrated accurately.

The second method does not require the buoy positioning, but it is not a simple matter to weigh precisely a sample cell with attached fill lines.

The magnetic densimeter we present here uses a third method in which the support coil, instead of the cell, is weighed. It is free from the disadvantages of the above two methods, and provides a method to measure the density of pressurized liquids easily and quickly. The method was first developed by the present author and his coworkers in 1981, and a system was built at NIST. The basic principles, and comparisons with conventional methods, are described in references [3, 4]. It has not been used for practical purposes, however, because an undesirable interaction between the buoy and a neighboring component was observed which killed the advantages of the new method.

Here, we present a brief description of further development of the densimeter. We built a new magnetic densimeter of the same type at the National Research Laboratory of Metrology, Tsukuba. After several improvements, we found the system worked as it was originally intended to in the temperature range 20-150 °C and pressure range 0-30MPa.

As an example of measurement, we present measurements of toluene density, which we carried out as part of an inter-laboratory comparison program between six groups in NRLM, NEL, NIST and PTB.

2 Principle of operation

Figure 1 illustrates the principle of the present densimeter. A small field coil hangs from a balance and surrounds a cylindrical cell. The cell contains a pressurized sample liquid and a buoy which is a permanent magnet. The purpose of this configuration is to enable a precise weighing of the buoy encapsulated in the pressure cell using a balance placed outside of the cell. It is then possible to measure the density of pressurized liquids in a way similar to ordinary hydrostatic weighing.

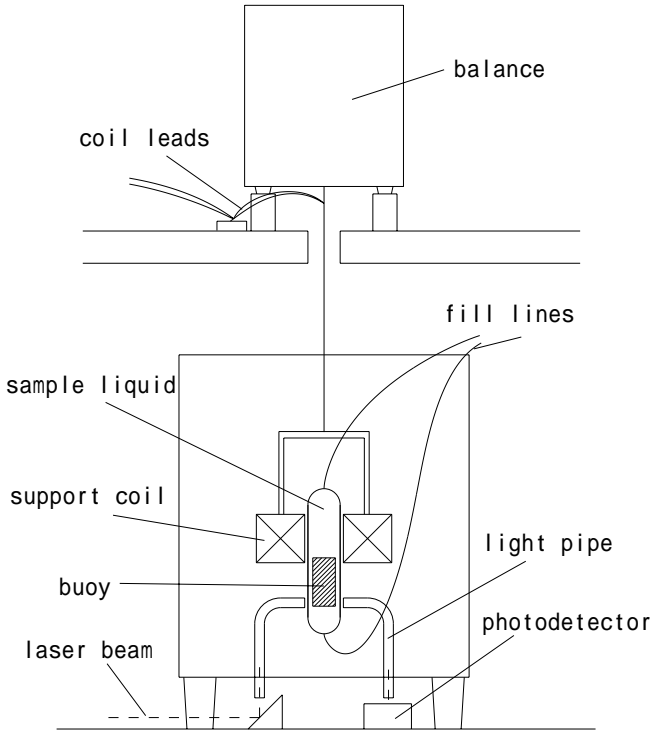


Figure 1: Principle

When there is no current in the coil, the buoy rests on the bottom of the cell, and the balance indicates the weight of the coil only. When the coil current is activated and the buoy is in support, the balance indicates the weight of the coil plus the apparent weight in the sample of the buoy. Therefore the apparent weight of the buoy (F) is measured directly as a change in the balance reading as the buoy is brought into support. The density of the sample, ρ , is obtained using the relation

$$F = (m - \rho V)g, \quad (1)$$

where m and V are mass and volume of the buoy, and g acceleration due to gravity.

Due to the nature of the magnetic field, a feedback control is necessary for stable support of the buoy. The present densimeter uses an optical sensing system which senses the vertical position of the buoy. The output signal from it controls the coil current electronically, so that the buoy is supported in a stable position.

3 Apparatus

In this section, we will describe the major components of the densimeter. The description will be focused mainly on the improvements over the previous design[3, 4].

The balance The balance used was an electronic balance which had a capacity of 200g and a resolution of 0.01mg. The beam of such a balance does not deflect on loading. This feature is essential for this application, in which we have a coil suspended from the balance whose leads have to be connected to an external current supply. Since there is no perceptible vertical motion of the coil, there is no elastic deformation in the coil leads; hence undesirable elastic force, which would otherwise destroy the balance sensitivity, is eliminated.

Since the sensitivity of an electronic balance can change with time, we built a computer-controlled calibration system which used a five-gram ring weight that had been calibrated against our standard weights. The balance was calibrated automatically before and after each measurement session.

The cell The sample cell consisted of a synthesized sapphire tube of 11.7mm O.D., 8.5mm I.D., and 94mm length. Sapphire was chosen for high fracture strength at high pressures and good transparency for use with an optical sensing system. To avoid fractures due to sharp stress concentrations, the sapphire tube was mounted in such a manner that it contacted only soft teflon components(Fig.2).

Pressure tests confirmed that, at 200 °C , the sapphire tube could take 40MPa, which was the maximum pressure attainable with our diaphragm pump. In fact, the O-rings and

the teflon components were damaged first.

The sapphire tube was coated with yttrium oxide for better conductivity both inside and outside to discharge static electricity.

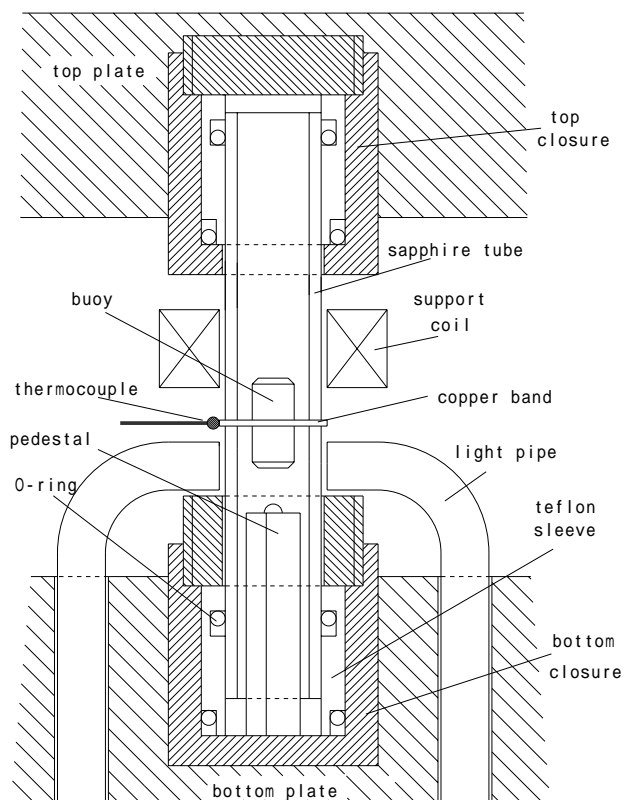


Figure 2: The sample cell. The top and bottom plates are tied together with two titanium rods to hold the pressure.

Buoy and pedestal The buoy was a strong neodymium magnet coated with nickel (Fig.2). It had a cylindrical shape 7mm in diameter and 15mm long, chamfered on both ends for protection against chipping. The nickel coating has strong resistance to corrosion in water, which enabled in-situ measurements of the buoy volume using water as a sample.

When the buoy is not in support, it sits on a pedestal placed on the bottom of the cell. The pedestal is made of a bundle of soft gold tubes to prevent chipping of the buoy when it falls on it.

Our previous densimeter had one difficulty, that after a few months of use, a magnetic interaction developed

between the buoy and the pedestal. The gold pedestal appeared to have ‘magnetized’, causing a height dependence of the buoy weight, which killed the major advantage of this method over Beams’ first method. The same magnetization occurred if gold was replaced with tin. Removal of it required disassembly of the cell and the thermostat and replacement of the pedestal. This problem hampered practical use of this densimeter.

In the early 90’s, we built a new densimeter of the same type at the National Research Laboratory of Metrology, Tsukuba. Further investigations using it showed that the

magnetic buoy handled in an ordinary laboratory environment had a lot of fine magnetic particles on the surface. Traces of this material were transferred to the gold pedestal after repeated dropping of the buoy onto it. We further found that the transfer of these particles could be prevented by covering the top of the pedestal with a harder metal such as copper.

Furthermore, we found that the particles turned to greyish powdery material (probably oxides) when we kept the buoy in water at 150 °C and 30MPa for several hours. The powder appeared less magnetic and could be removed easily by wiping with an alcohol-dipped swab. The present apparatus uses a buoy cleaned in this way and a copper-topped pedestal. No magnetic interaction has been observed since this improvement.

The coil and the suspension system In order to minimize the heating of the sample due to dissipation from the coil, the coil dimension was optimized so that the maximum magnetic force was obtained with minimum heat dissipation[3]. The winding of the present coil had 16mm I.D., 28mm O.D. and 13mm thickness. Its power consumption was 0.3W when it supported the buoy in vacuum. The wire had polyimide coating for insulation for use at temperatures above 200 °C . The coil leads were flexible silver wires. They were drawn out from the suspension system at a point near the balance bottom, and connected to an external current supply (Fig.2).

Feedback control In order to bring the buoy to a stable support, the densimeter used a feedback control of the coil current. It used an optical system for position sensing.

A He-Ne laser beam was introduced into the cell through a fiber-optic light pipe. The light pipe penetrates the bottom wall of the thermostat and the bottom plate of the cell assembly. After the beam passes through a clearance under the supported buoy, another light pipe takes it out from the cell and guides it to a photodiode placed outside the thermostat. The height of the buoy is represented by the intensity of the output light, which is converted to a voltage by the diode. The voltage signal is processed by a control circuit and used to control the coil current.

For convenience of handling, the light pipe was divided into three sections, each pen-

etrating the insulation wall, the thermostat bottom and the bottom plate of the cell. They were aligned to each other at the same time the cell and the thermostat were assembled.

Alignment of the axis The buoy and the coil were aligned with the sapphire tube so that there was no mechanical contact between them. A slight deformation of the cell frame took place, however, when pressure was applied to the sample. In order to give an allowance for the displacement of the cell wall, it was desirable to support the buoy as close to the center of the cell as possible. To achieve this, the balance was placed on a precise xy-table that had no backlash. The absolute xy-coordinates of the balance were indicated on dial gauges with a resolution of $10\text{ }\mu\text{m}$.

We took the axial alignment in the following way. The balance was moved in small steps in the, say, $+x$ direction. When the buoy reached the cell wall, a large change was observed in the balance reading. We recorded the x -coordinate of the position indicated on the dial gauge. We did the same thing in the $-x$ direction, and then the balance was brought to the middle of the two recorded positions. The entire procedure was repeated in the y -direction. In this way, the buoy was brought to the center of the sapphire tube. This procedure could be carried out even when viewing of the cell inside was not possible (e.g. when the thermostat was hot).

Temperature control and measurement The thermostat was a thick aluminum cylindrical vessel 121mm I.D., 160mm O.D. and 290mm high. Thin parallel grooves were cut in the axial direction into the outer surface of the cylinder, and heater wires enclosed in thin stainless steel tubes were embedded in them. An inductance bridge using a thermistor was used for the temperature control.

Two walls filled with 60mm thick ceramic fiber layer were used for heat insulation. The walls were two half-cylinders cut in the axial direction so that the insulation was achieved by placing them on both sides of the aluminum cylinder. Two circular disks of a similar structure were placed on the top and the bottom of the thermostat. The top disk was split to permit access for the suspension wire.

The present densimeter uses an air thermostat as opposed to the silicone oil bath in the previous design[3, 4]. We found that temperature equilibrium was attained quickly enough even if we did not have the oil in the thermostat. It is because the sample volume takes only a very small portion (less than 10 cm^3) of the total thermostat volume ($3,300\text{ cm}^3$).

A temperature gradient was observed to develop in the sample. With this densimeter, however, it was easy to remove it, because the sample could always be stirred using support/drop motions of the buoy.

Another problem with the air thermostat is temperature measurement. Because of the poor thermal contact, it is essential to place the sensor in direct contact with the sample. A platinum resistance thermometer calibrated at NRLM was mounted in a hole drilled in a thick aluminum block which was a part of the cell frame. A copper-constantan thermocouple was used to measure the temperature difference between the PRT and the cell. The cell had a thick copper band wound around it, and one side of the thermocouple was soldered to it. The other side of the thermocouple was inserted in a hole drilled close to the PRT. Since constantan contains nickel, which is magnetic, the copper band was placed at a position at the middle of the levitated buoy so that the magnetic interaction between the buoy and the constantan became negligible. The thermocouple leads were drawn out in a direction perpendicular to the cell axis.

The stability of temperature control was $3\text{mK}/10\text{h}$ at $50\text{ }^\circ\text{C}$, $10\text{mK}/10\text{h}$ at $100\text{ }^\circ\text{C}$ and $20\text{mK}/10\text{h}$ at $150\text{ }^\circ\text{C}$. The maximum temperature difference detected by the thermocouple was 1.6K at $150\text{ }^\circ\text{C}$. When the sample temperature was changed, a new temperature equilibrium was reached typically in four hours.

Pressure measurement We measured pressure using quartz pressure gauge which had a capacity of 40MPa and an accuracy of 0.01% of reading. The gauge was calibrated by the manufacturer against the DH primary pressure standard, Model-5306, which was traceable to an NIST standard.

4 Measurement of the density of toluene

4.1 Method

We determined the volume of the buoy (V) as a function of temperature and pressure by weighing the buoy in water at 27 points in the range 24-150 °C and 0.1-30MPa. We used The New Scientific Formulation of IAPWS to calculate the density of water. A linear function of both temperature and pressure was least-square fitted to the volume data.

The toluene sample was purified and supplied by NIST(Boulder) for the inter-laboratory comparison. Measurements were performed on nine isotherms in a sequence, 24, 40, 60, 80, 100, 90, 70, 50 and 30 °C , at six pressures, 0.1, 1, 5, 10, 20 and 30MPa. Three additional isotherms, 30, 100 and 40 °C , were measured at pressures 0.1, 10, 20, 30MPa for replication. A measurement session at one point consisted of 15 series, each consisting of 12 cycles of buoy support/drop operations. A session took approximately one hour. Measurement of one isotherm took a day. The balance was calibrated before and after each measurement session.

We carried out two in-vacuum weighings of the buoy, one before the in-water measurements, and one before the in-toluene measurements. The results of these two weighings were in agreement to 0.02 mg, indicating that the mass of the buoy was sufficiently stable. Using the mean of these values as the true mass of the buoy (m), the density was calculated using eq. (1).

4.2 Results

Table 1 lists the measurement results. We fitted the following function to the density data using the least-square method. This function was devised by Watson [5] who used it to represent the density data of toluene measured by Magee and Bruno[6].

$$\begin{aligned} \rho = & A1 + tr2 \times (tr0p5 \times (A2 + A4 \times tr + A5 \times tr10) + A3 \times tr) + A6 \\ & \times \sqrt{pr} \times tr10 + pr \times tr \times (A7 + A8 \times tr3 + pr \end{aligned}$$

$$\times tr2 \times (A9 \times tr0p5 + A10 \times pr3 \times tr2)),$$

where

$$tr = (t + 273.15)/300,$$

$$pr = p/10,$$

$$pr3 = pr^3,$$

$$trn = tr^n (n = 2, 3, 5, 10),$$

$$tr0p5 = tr^{0.5}.$$

The coefficients obtained are:

A1	9.401 005 887 20 $\times 10^{-1}$	A2	1.113 660 103 96
A3	-2.234 237 682 69	A4	1.041 633 480 31
A5	-5.538 170 928 45 $\times 10^{-4}$	A6	7.541 077 161 24 $\times 10^{-5}$
A7	6.045 551 523 31 $\times 10^{-3}$	A8	2.098 433 109 08 $\times 10^{-3}$
A9	-3.181 224 081 03 $\times 10^{-4}$	A10	3.352 208 948 68 $\times 10^{-7}$

Comparisons with other participants of the inter-laboratory comparison are not available, because the program has not been completed at the time of writing. Table 2 compares the values calculated using this equation with Watson's formulation[5] of Magee and Bruno data[6].

4.3 Uncertainties

The residuals of the fitting were regarded as random fluctuations, the RMS of which was 0.16kg/m³. The systematic part of the uncertainty was as follows.

The five-gram ring weight used for balance calibration was calibrated against our standard weights to an accuracy of 35 μ g.

The pressure gauge is traceable to NIST standards to an accuracy of 0.01%.

One of the difficulties in the method employed here is the temperature drift occurring in the sample. This is caused by dissipation from the coil. The drift amounted to 0.2K

during a one-hour measurement session. Since the speed of response of the thermocouple was sufficiently fast (15-20s), the temperature difference between the thermocouple and the cell due to retardation was negligible. The temperature gradient within the cell was assumed to be negligible, because the sample was stirred by the frequent support/drop operation of the buoy which was a part of the measurement procedure itself. In one measurement session, we measured temperature six times in 12-minute interval. The mean of these measurements was found to represent the true mean temperature to an accuracy of 0.005K. Together with the PRT calibration error (0.003K at 100 °C), the total systematic error in temperature measurement was estimated to be 0.006K.

The function representing the buoy volume had an uncertainty due to uncertainties in the parameters determined by least-square fitting. The maximum of such uncertainty was estimated to be 0.00008cm³. The uncertainty involved in the NSF formulation was negligible.

The toluene sample was carefully purified at NIST. We transferred it into the densimeter in vacuum. The densimeter was first cleaned by toluene at 150 °C . We therefore assumed that the contribution from impurities was negligibly small.

The following table summarizes the uncertainties of the measurement.

Error factors	Uncertainties	Uncertainties in density	
		(kg/m ³)	(%)
random		0.16	0.019
systematic			
balance calibration	35μg	0.007	0.001
temperature	0.006 K	0.006	0.0007
pressure	0.003 Mpa	0.003	0.0004
buoy volume	0.00008 cm ³	0.12	0.014
impurity	≈ negligible	0	0
combined standard uncertainty		0.20	0.024

5 Conclusions

We conclude that a magnetic-suspension densimeter in which the support coil is suspended from a balance can measure densities of pressurized liquids with an accuracy of a few hundredths of a per cent. Since the densimeter does not need accurate positioning of the buoy with respect to the coil, the measurement procedure was simple and rapid; most of it was automated. Measurement of the density of toluene showed that the results agreed with reliable literature values within the claimed accuracy in all the measurement range.

Acknowledgements

This work was based on a collaboration at NIST with J.M.H. Levelt Sengers, W.M. Haynes, R.F. Chang and H. Davis. T.J. Bruno prepared the toluene sample for the inter-laboratory comparison, which was organized by J. Watson and M. McLinden. The sample fill system used in this work was a modified version of what W.M. Haynes suggested to the author. A. Ono and K. Fujii took care of funding and other managerial matters for this project. H. Monden provided us with valuable suggestions on machining of the high pressure components.

References

- [1] J.W. Beams, C.W. Hulburt, W.E. Lotz, Jr., and R.M. Montague, Jr., *Rev. Sci. Instrum.* **26**, 1181 (1955)
- [2] J.W. Beams and A.M. Clarke, *Rev. Sci. Instrum.* **42**, 1455 (1971)
- [3] R. Masui, W.M. Haynes, R.F. Chang, H.A. Davis and J.M.H. Levelt Sengers, *Rev. Sci. Instrum.* **55**(7), 1132 (1984)
- [4] R. Masui, H.A. Davis and J.M.H. Levelt Sengers, *Proceedings of the Eighth Symposium on Thermophysical Properties* **1**, 128 (1982)

[5] J. Watson, private communications

[6] J.W. Magee and T.J. Bruno, J. Chem. Eng. Data **41**, 900 (1996)

Table 1. Results

temperature (°C)	pressure (MPa)	density (kg/m ³)		
		measured	calculated	residuals
24.832	30.158	884.16	884.13	0.03
24.974	19.778	877.22	877.17	0.05
25.044	9.988	870.47	870.09	0.38
25.042	5.127	866.47	866.39	0.08
25.016	1.133	863.30	863.24	0.06
24.982	0.164	862.29	862.48	-0.19
41.532	30.069	870.38	870.33	0.05
41.540	19.945	863.09	863.10	-0.01
41.586	10.016	855.45	855.30	0.15
41.605	5.085	851.34	851.14	0.20
41.609	1.086	847.53	847.63	-0.10
41.606	0.175	846.59	846.81	-0.22
60.987	19.583	845.66	845.91	-0.25
61.048	29.790	853.82	853.88	-0.06
61.024	10.009	837.06	837.55	-0.49
61.020	5.145	832.93	832.98	-0.06
61.023	1.063	828.94	828.94	-0.01
61.013	0.168	828.07	828.02	0.04

Table 1. Results (continued)

temperature (°C)	pressure (MPa)	density (kg/m ³)		
		measured	calculated	residuals
79.321	30.108	838.85	839.04	-0.19
79.318	19.773	830.15	830.17	-0.02
79.531	10.062	820.58	820.64	-0.06
79.612	5.107	815.27	815.36	-0.09
79.661	1.111	810.91	810.87	0.05
79.679	0.176	809.97	809.74	0.23
100.461	30.064	821.85	821.84	0.02
100.341	19.914	812.30	812.22	0.08
100.307	10.070	801.50	801.60	-0.09
100.313	5.142	795.68	795.72	-0.04
100.317	1.085	790.42	790.53	-0.11
100.328	0.180	788.97	789.26	-0.29
89.474	30.104	830.80	830.77	0.03
89.507	19.976	821.51	821.59	-0.08
89.523	10.166	811.66	811.60	0.06
89.527	5.182	805.87	806.05	-0.18
89.534	1.051	801.23	801.13	0.10
89.531	0.176	800.19	800.01	0.17
70.291	30.272	846.70	846.59	0.10
70.298	19.988	838.11	838.16	-0.06
70.297	10.118	828.99	829.15	-0.16
70.307	5.094	824.23	824.16	0.07
70.305	1.017	819.95	819.88	0.07
70.310	0.165	819.18	818.93	0.26

Table 1. Results (continued)

temperature (°C)	pressure (MPa)	density (kg/m ³)		
		measured	calculated	residuals
51.858	29.958	861.82	861.66	0.16
51.854	20.113	854.30	854.29	0.01
51.856	10.130	846.19	846.05	0.14
51.865	5.094	841.68	841.56	0.12
51.868	1.064	837.87	837.79	0.08
51.871	0.175	837.07	836.92	0.15
30.245	30.140	879.54	879.70	-0.15
30.228	20.011	872.86	872.87	-0.01
30.213	10.042	865.55	865.55	0.01
30.235	5.066	861.73	861.62	0.11
30.280	1.045	858.16	858.28	-0.12
30.255	0.172	857.35	857.57	-0.22
30.184	0.179	857.43	857.64	-0.22
30.233	9.990	865.50	865.49	0.01
30.241	20.003	872.89	872.85	0.03
30.243	30.119	879.54	879.68	-0.15
100.266	29.906	821.89	821.85	0.04
100.363	20.021	812.53	812.31	0.22
100.307	10.157	801.71	801.70	0.01
100.354	0.175	789.34	789.22	0.12
41.824	0.132	846.46	846.56	-0.10
41.828	10.027	855.22	855.09	0.13
41.851	20.027	862.99	862.90	0.10
41.883	30.053	870.04	870.03	0.01

Table 2. Comparison with J.W.Magee and T.J.Bruno's data as formulated by J. Watson[5]

temperature °C	pressure MPa	MBW equation kg/m ³	present meas. kg/m ³	diff. kg/m ³
25.000	0.100	861.90	862.41	-0.51
25.000	10.000	869.43	870.14	-0.71
25.000	20.000	876.48	877.30	-0.82
25.000	30.000	883.05	883.89	-0.84
40.000	0.100	847.81	848.27	-0.47
40.000	10.000	856.04	856.72	-0.68
40.000	20.000	863.68	864.48	-0.80
40.000	30.000	870.73	871.55	-0.82
60.000	0.100	828.76	828.94	-0.18
60.000	10.000	838.10	838.48	-0.38
60.000	20.000	846.60	847.11	-0.52
60.000	30.000	854.38	854.91	-0.53
80.000	0.100	809.27	809.33	-0.06
80.000	10.000	819.93	820.15	-0.22
80.000	20.000	829.44	829.79	-0.34
80.000	30.000	838.06	838.40	-0.34
100.000	0.100	789.06	789.46	-0.40
100.000	10.000	801.37	801.80	-0.43
100.000	20.000	812.09	812.60	-0.51
100.000	30.000	821.69	822.15	-0.46